This is to certify that the

thesis entitled

PREDICTING SHOCK TRANSMISSION CHARACTERISTICS FOR RIBBED EXPANDED POLYPROPYLENE CUSHIONS USING STANDARD CUSHION CURVES FOR FLAT PLANK CUSHIONS

presented by

GARY CARLTON GRANTHEN

has been accepted towards fulfillment
of the requirements for

M. S. degree in PACKAGING

Gary Burgess
Major professor

Date MAY 2, 1991

PREDICTING SHOCK TRANSMISSION CHARACTERISTICS FOR RIBBED EXPANDED POLYPROPYLENE CUSHIONS USING STANDARD CUSHION CURVES FOR FLAT PLANK CUSHIONS

By

Gary Carlton Granthen

A THESIS

Submitted to
Michigan State University
in partial fulfillment of the requirements
for the degree of

MASTER OF SCIENCE

School of Packaging

1991

ABSTRACT

PREDICTING SHOCK TRANSMISSION CHARACTERISTICS FOR RIBBED EXPANDED POLYPROPYLENE CUSHIONS USING STANDARD CUSHION CURVES FOR FLAT PLANK CUSHIONS

BY

GARY CARLTON GRANTHEN

This study examines seven different mathematical models which predict the peak deceleration G in dynamic loading of 1.9 PCF ribbed expanded polypropylene cushions. Each method is based on converting the ribbed cushion into an equivalent plank cushion so that published cushion curve data can be used to determine G. Three drop heights of 18", 30" and 42", three rib angles of 5°, 15°, and 25°, three static loadings, and three rib heights of 1.5", 2.0" and 2.5" were tested.

The results show that the Equivalent Volume method which weighs the varying cross sectional areas of the ribbed portion and the plank portion of the cushion equally, best predicts G. This newly calculated "bearing area" based on this method can then be used to calculate the static stress which in turn can be used to determine the peak deceleration from the standard cushion curves. This model is shown to rest on solid physical grounds through an examination of the resistance to compression using the Gas Law.

ACKNOWLEDGMENTS

I wish to thank Dr. Paul Singh and Dr. George Mase for their support and helpful suggestions while serving on my Graduate Committee. I also wish to thank Joseph Franklin of ARCO CHEMICAL COMPANY for his guidance and material donation that made this whole project possible. A very special thanks goes to Dr. Gary Burgess for his time, patience, good humor, and guidance while acting as my advisor and helping me through the difficult times. I am deeply indebted and forever appreciative.

TABLE OF CONTENTS

LIST OF TABLES

LIST OF FIGURES

CHAPTER 1

INTRODUCTION AND LITERATURE REVIEW

Selecting the best type and amount of cushioning for a particular packaging application depends on only three or four variables in most instances. There are some general procedures that may be applied so that the process of designing a cushion for a fragile item need not be very complicated [Hanlon, 1971]. Unfortunately, these procedures are limited to plank type cushions which often do not offer the most economical protection. The purpose of this research is to extend these procedures to include designing ribbed cushions using published data for plank cushions.

Rational cushion design requires the consideration of many factors. The procedure for cushion design as outlined in MIL - HDBK - 304B (1978) is as follows:

Part 1. Determine all pertinent elements of the problem. These include items such as product weight, size and shape, the expected drop height, and product fragility.

Part 2. Determine the most economical cushioning material for protection of the product.

Part 3. Estimate the allowance in thickness of cushioning pads that is required to offset creep.

Part 4. Calculate the exterior container dimensions.

Part 5. Perform impact tests to verify package design.

One of the considerations in Part 1 is the type of distribution environment the package is likely to encounter such as whether it is shipped by truck, rail, boat, air or combinations of these and how it is handled (forklifts, cranes etc.) Table 1 may be used to establish an expected drop height for the package if the weight is known [ASTM Std. D 3332 - 88].

TABLE 1. Expected drop height versus package weight.

Package weight, pounds	Type of handling	Drop height, inches
0 - 20	1 man throwing	42
21 - 50	1 man carrying	36
51 - 250	2 men carrying	30
251 - 500	Forklift truck	24
501 - 1000	Forklift truck	18
1000 - Up	Forklift truck	12

Another consideration in Part 1 is determining the fragility of the product. The fragility of the product can be determined by performing drop tests on a shock machine and constructing a damage boundary curve [ASTM STD. D 3332 - 88] as in Figure 1.

The product is first subjected to a series of very short, constant duration shocks from greater and greater drop heights until it breaks. The critical velocity change for the product is recorded as the area under the shock pulse which just causes damage to the product. In theory, the product will be able to endure shocks of any amplitude (peak

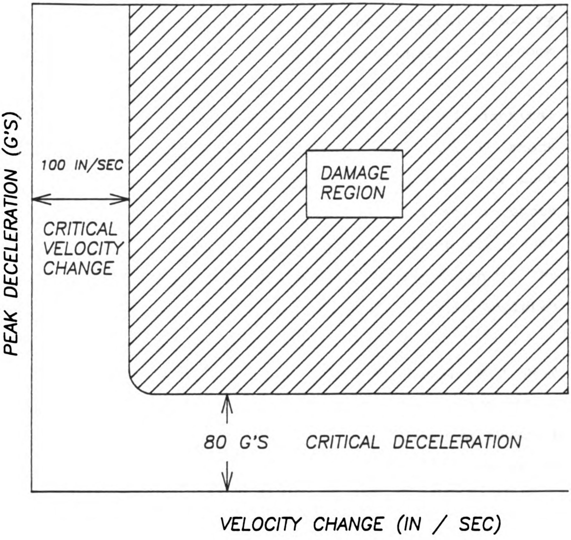

FIGURE 1. DAMAGE BOUNDARY CURVE.

deceleration) as long as the velocity change for the shock is less than this critical velocity change for the product. The actual velocity change in any drop may be estimated from the expected drop height in Table 1 as the sum of the impact velocity and the rebound velocity. When the velocity change for any other shock is greater than the critical velocity change for the product, the product becomes sensitive to shock amplitude [Newton 1968].

Another drop test on a shock machine using an identical new product is required to determine the critical shock amplitude. The product is now subjected to a series of much longer duration shocks with steadily increasing shock amplitudes until it breaks. The peak deceleration which just causes damage is recorded as the critical acceleration for the product, also loosely called its fragility. This completes the damage boundary picture in Figure 1.

In theory, any shock whose velocity change and peak deceleration are such that they fall within the damage region will cause the product to break. As a consequence of this, if the velocity change that a product is expected to encounter in a drop is less than the critical velocity change for the product (from the damage boundary curve), then no cushioning is needed in the package since the primary protective function of the cushion is to limit the peak deceleration and the peak deceleration is irrelevant in this situation. It is usually the case however that the velocity change exceeds this value so that a cushion is needed to keep the peak deceleration less than the critical deceleration (from the damage boundary curve).

Once the product fragility is known, there are many types of cushioning materials which may be used in Part 2 of the MIL-HDBK cushion design procedure. Cushions may be divided into two categories based on structure: open cell and closed cell foams. In general, closed cell (trapped air) foams are stiffer and therefore produce higher G's than open cell (air flow) foams. Closed cell foams are capable of supporting much heavier products however. The dynamic performance for many of these materials is published in the form of cushion curves where the peak deceleration is plotted on the ordinate (y-axis) against static stress on the abscissa (x-axis) as in Figure 2. It is important to note that all published curves are for plank type cushions (uniform thickness) only. It also should be noted that each of the cushions curves in Figure 2 go through a minimum at some static stress. At the low static stress end, a high peak-G is obtained because there is insufficient energy to compress the cushion. At the high static stress end, a high peak-G is also obtained because the cushions "bottoms out" in an attempt to absorb the excess free fall energy [Benning, 1969]. At some static stress in between these limits, the peak-G is lowest.

42" DROP

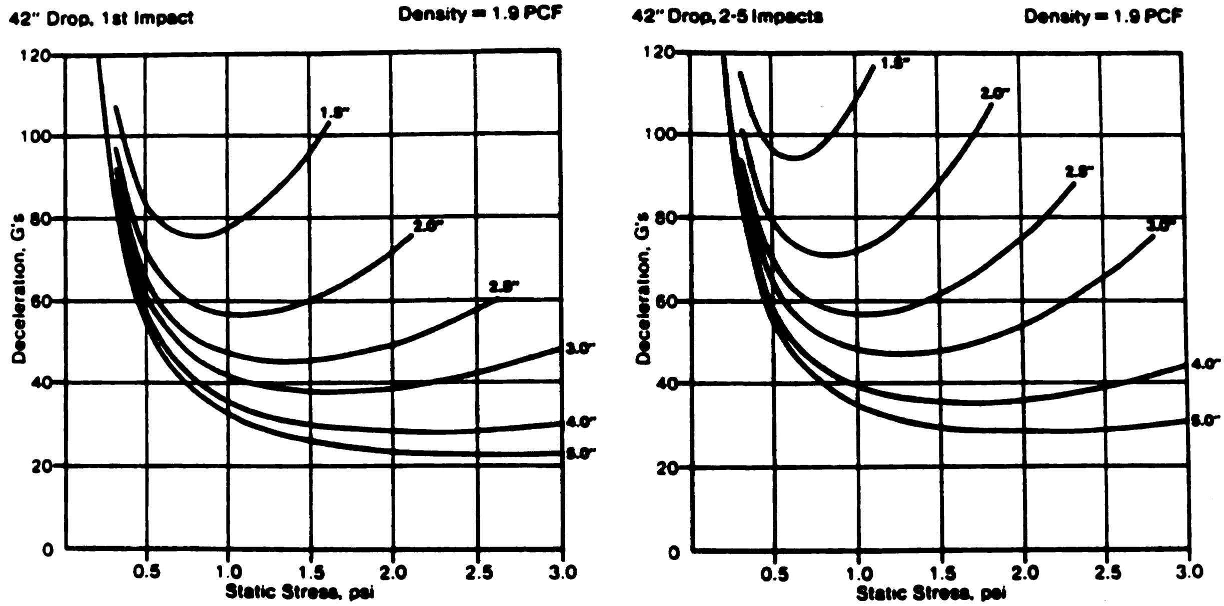

36" DROP

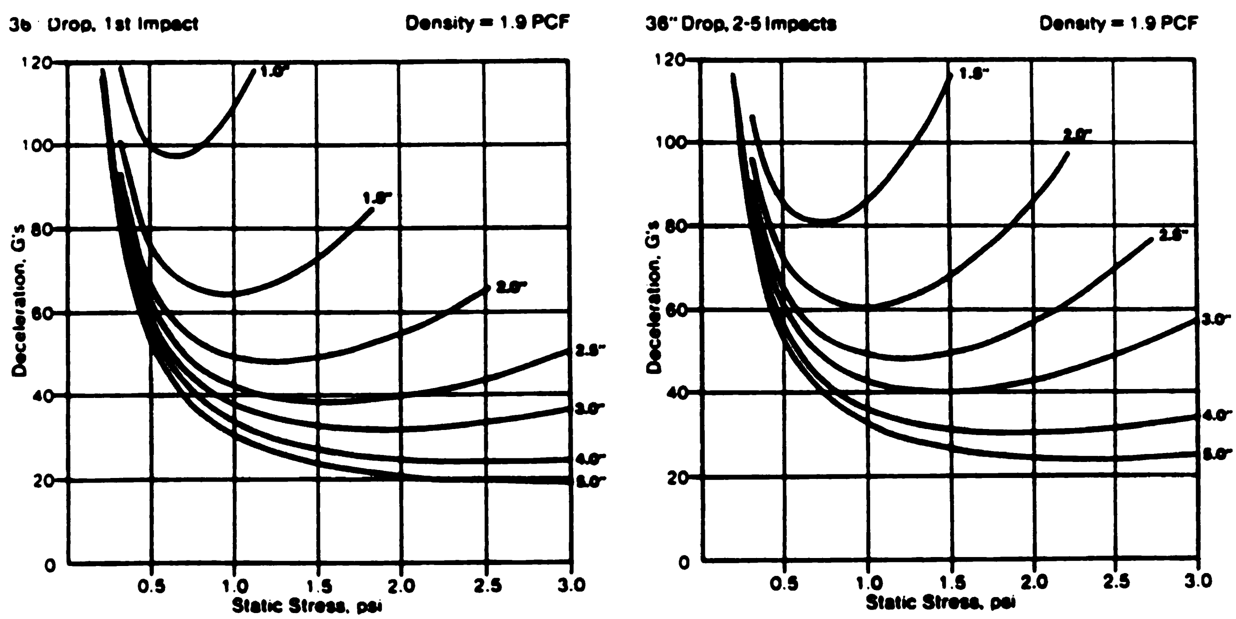

Figure 2. Cushion curves for ARPRO® 3319 EPP BEAD.

30" DROP

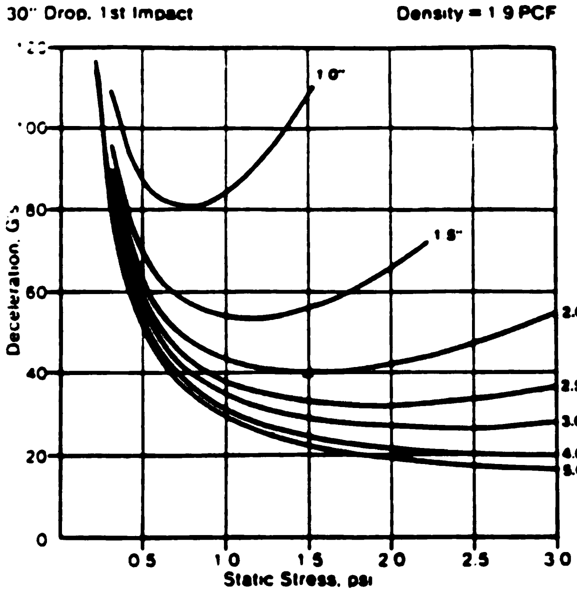

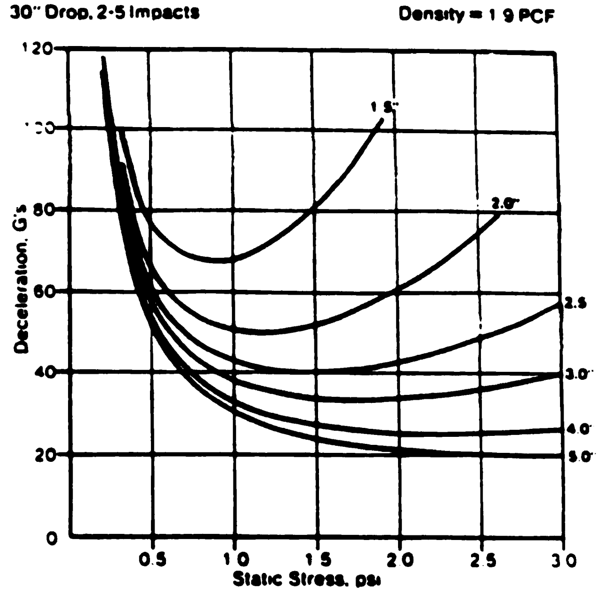

18" DROP

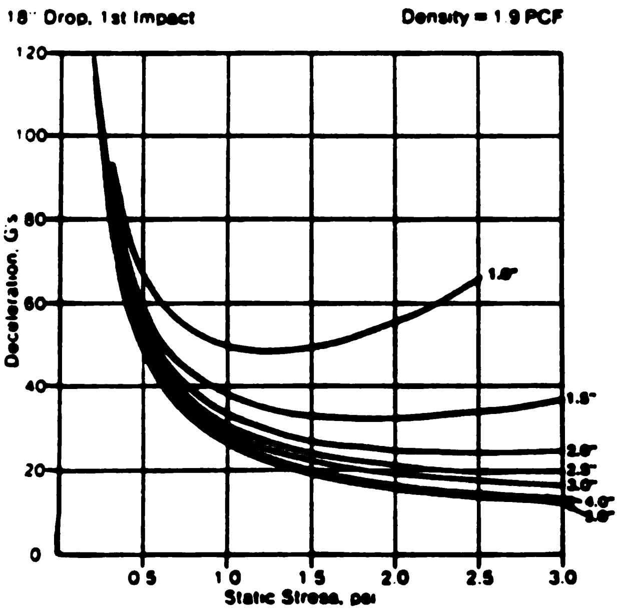

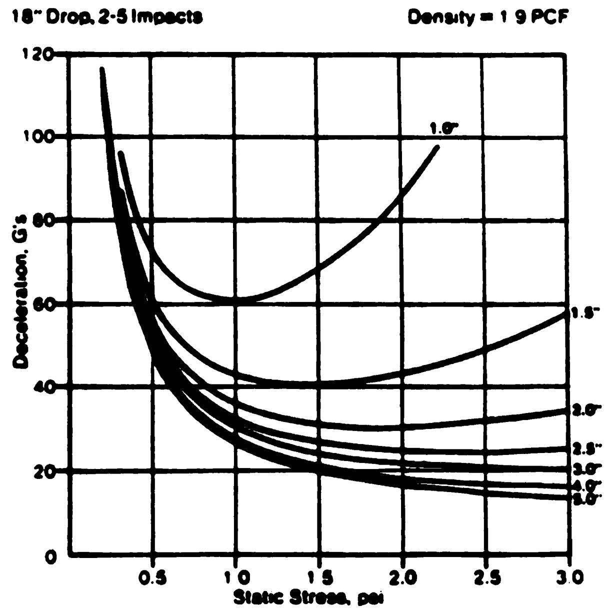

Figure 2. (cont'd.)

If the cushion is designed as a simple rectangular flat plank, the static stress σ referred to in the cushion curves is calculated as:

$$\sigma = W / A , \qquad \text{Equation (1)}$$

where **W** is the weight of the product and **A** is the bearing area between the product and the cushion. To determine the correct amount of cushioning required to protect the product, the following approach is normally used in Part 2 of the MIL-HDBK procedure:

Step 1. Determine first whether or not the product needs a cushion. Use Table 1 to estimate the expected drop height and calculate the maximum possible velocity change for this height as the maximum:

$$\Delta V = 2\sqrt{2gh}. \qquad \text{Equation (2)}$$

If this is less than the critical velocity change for the product from the damage boundary curve, then the product does not need a cushion. If it is greater than the critical velocity change, then continue with Step 2.

Step 2. Select a particular type of cushion for the expected drop height. The selection should be based on economy and protective ability.

Step 3. Decide on the area **A** under which the product is to be supported and calculate the static stress $\sigma = W / A$.

Step 4. Select the minimum thickness that will limit the G-level to the fragility rating for the product determined from the damage boundary curve. It is recommended that the bearing area be greater than $(1.33 \text{ X thickness})^2$ to prevent the buckling situation shown in Figure 3.

This procedure will now be applied to a hypothetical situation in order to illustrate the method and to establish the need for being able to handle ribbed cushions.

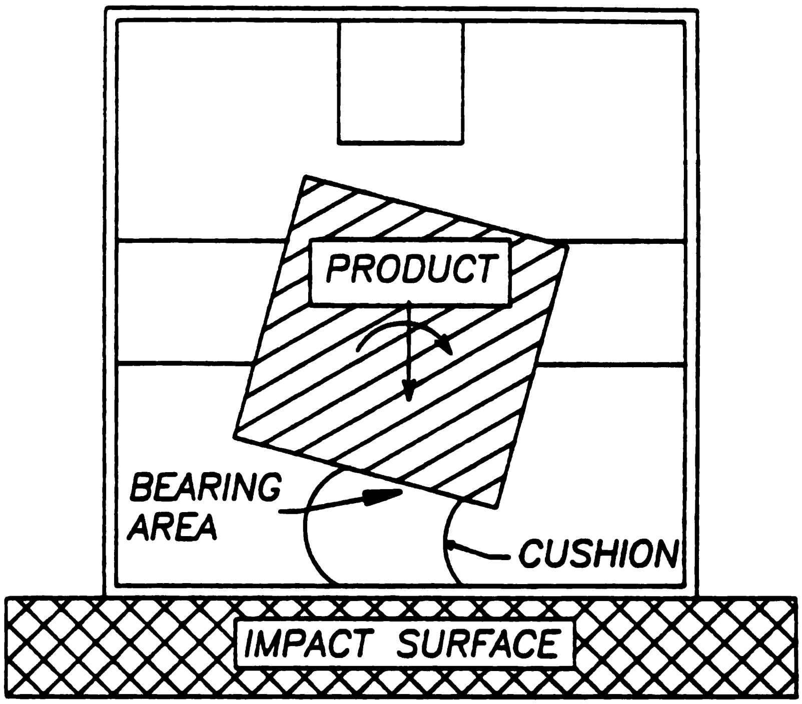

FIGURE 3. BUCKLING ASSOCIATED WITH A BEARING AREA THAT IS TOO SMALL.

EXAMPLE 1: A sensitive electronic product measures 8" X 8" X 6" and weighs 32 pounds. The product must be supported under its entire base. The damage boundary curve for the product in Figure 4 is shown in Figure 1. Design a cushion for multiple impacts.

Step 1. From Table 1, the expected drop height is 36". The maximum possible velocity change is

$$2\sqrt{2 * 386.4 * 36} = 334\ inches/sec\ ,$$ which exceeds

the critical velocity change of 100 in/sec from the damage boundary curve. The product therefore needs a cushion.

Step 2. 1.9 PCF ARPRO® Expanded Polypropylene Bead was chosen for purposes of illustration. The cushion curves for this material are shown in Figure 2.

Step 3. Since the product will be supported under its entire base by the cushion, the bearing area is 8" X 8" = 64 in^2 and the static stress σ = 32 lbs / 64 in^2 = 0.5 psi.

Step 4. From the cushion curves in Figure 2 for a 36 inch drop and a static stress of 0.5 psi, the thickness of the cushion must be at least 2" in order to keep the shock less than the fragility limit of 80 g's from the damage boundary curve in Figure 1. The actual shock incurred is 72 G's. For this cushion thickness, the minimum bearing area which will prevent buckling is $(1.33 \text{ X } 2")^2$ = 7.1 in^2. Since the actual bearing area is 64 in^2, buckling is not a problem.

In the previous example, a total of 8" X 8" X 2" = 128 in^3 of cushion was required to protect the product. It is possible to reduce this amount considerably using a ribbed cushion as the next example shows.

EXAMPLE 2: Suppose now you have exactly the same product as in Example 1, but you want to reduce the amount of material used to make the cushion to decrease packaging costs.

Step 1. Again, from Table 1, it is determined that the product will need a cushion.

Step 2. ARPRO® 1.9 PCF cushioning is again chosen.

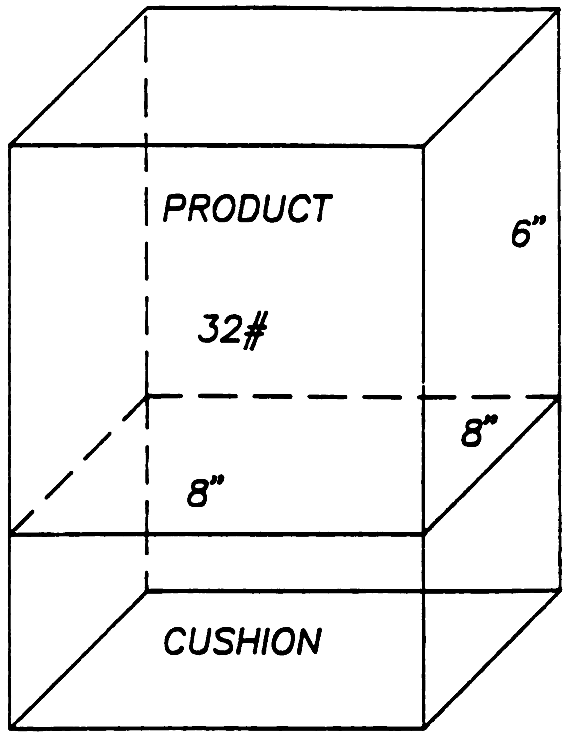

FIGURE 4. 32 POUND PRODUCT ON A PLANK CUSHION.

Step 3. If we temporarily relax the requirement that the product be supported under its entire base, the allowable bearing area may be determined from the cushion curves.

Using a 2" thick cushion, it is possible to maintain the same protection and use less material by increasing the static loading. The maximum static loading that can be used with a 2" thick plank of ARPRO® 1.9 PCF Expanded Polypropylene Bead without transmitting more than 80 G's in a 36" drop is 1.75 psi. In order to get a static loading of 1.75 psi, the bearing area must be reduced to 32 lbs / 1.75 psi = 18.3 in^2. The total amount of cushioning material is now 18.3 in^2 X 2 in = 36.6 in^3 , a considerable reduction in the 128 in^3 used in Example 1. Of course, this design is useless if we retain the requirement that the product be supported under its entire base since the bearing area of 18.3 in^2 for the plank cushion is less than the product base area of 64 in^2. The only way to maintain full base support and reduce the bearing area is to remove some of the load bearing material from the cushion as in Figure 5.

During impact, the force exerted downward on the top of the ribbed cushion by the product compresses the cushion which in turn absorbs energy and decelerates the product. At any instant, this force is essentially the same on every horizontal cross section of the cushion throughout its thickness. But, since the cross sectional area changes, the stress on each cross section is different which causes the cushion to deform more in thinner sections (at the feet). The

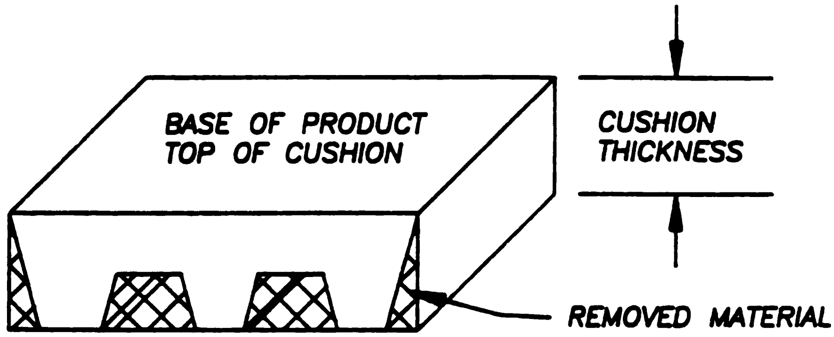

FIGURE 5. MATERIAL REMOVED FROM A PLANK CUSHION TO FORM A CUSHION WITH A NONUNIFORM CROSS SECTION.

cushion in Figure 5 therefore behaves like a smaller plank cushion with possibly a different thickness [Burgess, 1988]. The idea behind converting a cushion with a variable cross section into an equivalent plank cushion in terms of peak-G performance for purposes of analysis is central to this thesis since the primary objective is to be able to use published cushion curve data to predict ribbed cushion performance.

Before proceeding with ribbed cushion design, the remainder of the MIL - HDBK -304B cushion design procedure will be discussed. The motivation behind Part 3 of the cushion design procedure is that all cushions tend to lose thickness and thus reduce the protection they provide when subjected to a constant load for a period of time. This phenomenon is known as creep. The creep rate for most cushioning materials over time is greatest at initial loading and declines exponentially with elapsed time thereafter. Since the amount of settling is difficult to estimate exactly, it must be determined by testing. If it is known from experiment that in long term storage, a particular type of foam settles 5 percent for example, the design thickness for this type of cushion should be 100 / (1 - .05) = 105 % of the thickness chosen for protection from the cushion curves. Parts 4 and 5 of the cushion procedure are self explanatory and for this reason will not be covered here except to say that actual impact testing after design is especially recommended for ribbed cushions since the mode of deformation is much more complicated. For this reason, peak

G performance is expected to be much more approximate than for plank cushions.

To date, not much research has been done in the area of designing with ribbed cushions since the prediction of deceleration levels is difficult. For this reason, the survey shown in Appendix A was sent to a number of foam producers and users to evaluate the interest in these types of cushions. The applicants were asked to rank seven reasons for using ribbed cushions using a response of "1" as the most important reason to "7" as the least important. Table 2 shows the results of the survey. Reason 3 (Reducing G-levels for high product surface area situations), received 75 percent of the number 1 rankings while reason 5 (Better performance with less material), received the other 25 percent of the number 1 rankings. Reason 5 also received 57 percent of the number 2 rankings and 12.5 percent of the number 3 rankings. It would appear that reason 3 (Reducing G-Levels for high product surface area situations), and reason 5 (Better performance with less material), are the most popular responses.

TABLE 2. SURVEY

FREQUENCY OF VOTES (PERCENT)

RANKING

REASON NUMBER	1	2	3	4	5	6	7
1				40	33		
2			12.5	40	67		
3	75		12.5	20			
4		43	62.5				
5	25	57	12.5				
6							100
7						100	

REASONS

1. Ease of hand fabrication for short term production runs.
2. Ease of molding for long term production runs.
3. Reducing G-levels for high product surface area situations.
4. Lower cost than plank cushions for the same performance.
5. Better performance with less material.
6. Company requires you to.
7. Status Quo.

Chen [1986] studied the effect of ribbing on the shock transmission characteristics of expanded polystyrene cushion material using 3 different thicknesses, 6 different drop heights, and five different static stress levels. Side by side comparisons for both ribbed and flat EPS were presented. It was observed that at lower drop heights and static stresses, the shocks obtained from ribbed and flat EPS were similar, at higher drop heights and static stresses however, the cushion curves for ribbed and flat EPS differed significantly. It was concluded that the cushion curves developed for flat planks are inadequate to describe the cushioning behavior of ribbed EPS under more severe conditions.

Chen's study outlines the basic problem of designing ribbed cushions but does not offer a simple solution. It would be necessary to generate an infinite number of cushion curves to be able to predict the dynamic behavior for each possible cushion configuration because the dynamic response of the cushion is affected by the shape of the test specimen [Kerstner, 1957]. Kerstner also notes that using a rib taper of 5° to 15° also helps to reduce buckling. They [Kerstner, 1957; Pearsons and Ungar, 1961] point out that although economy of cushioning design might dictate the reduction of cushioning bearing area to a minimum, the designer must insure that the load bearing area portion of the item can withstand the resultant stress. It is the intent of this research to simplify the design of ribbed cushions by developing a method which will allow a ribbed cushion to be viewed as an equivalent plank cushion so that the shock transmitted may be estimated using the standard cushion curves.

CHAPTER 2

MATERIALS AND METHODS

2.1 MATERIAL

The cushion material used in this research was ARPRO® 3319 Expanded Polypropylene Bead with a density of 1.9 pounds per cubic foot. The material is a low density closed cell foam made by ARCO CHEMICAL COMPANY. Large planks were cut into 8" X 8" X 2" squares and two squares were then glued together with 3M 76™ High Tack Adhesive to form 8" X 8" X 4" planks. The hot wire and fixture with interchangeable guide plates in Figure 6 were used to cut consistent ribs into the planks as in Figure 7.

2.2 DESIGN OF EXPERIMENT

Three different rib heights (dimension b in Figure 7) of 1.0", 1.5", and 2.0" and three different rib angles (θ in Figure 7.) of 5°, 15°, and 25° for a total of 3 X 3 = 9 different cushion configurations were constructed. Figures 8 through 16 show the actual configurations that were used in the experiment. Three different loadings and three different drop heights of 18", 30", and 42" were chosen to simulate "average" conditions. Each cushion sample was randomly assigned a loading, drop height, and rib configuration and each data point was replicated 4 times for a total of 3 X 3 X 9 X 4 = 324 samples.

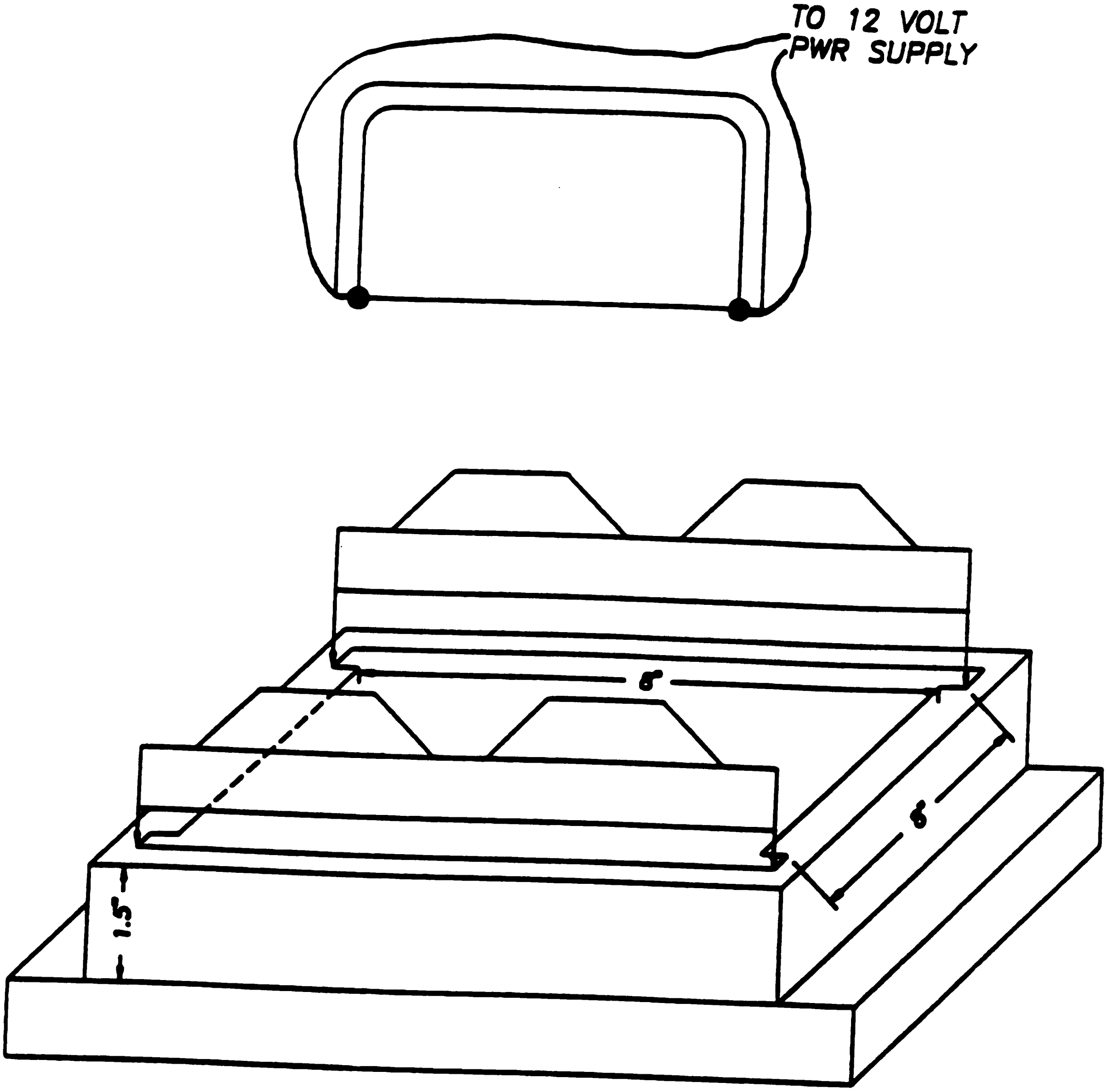

FIGURE 6. Hot wire and cutting fixture.

Depth = Width = e

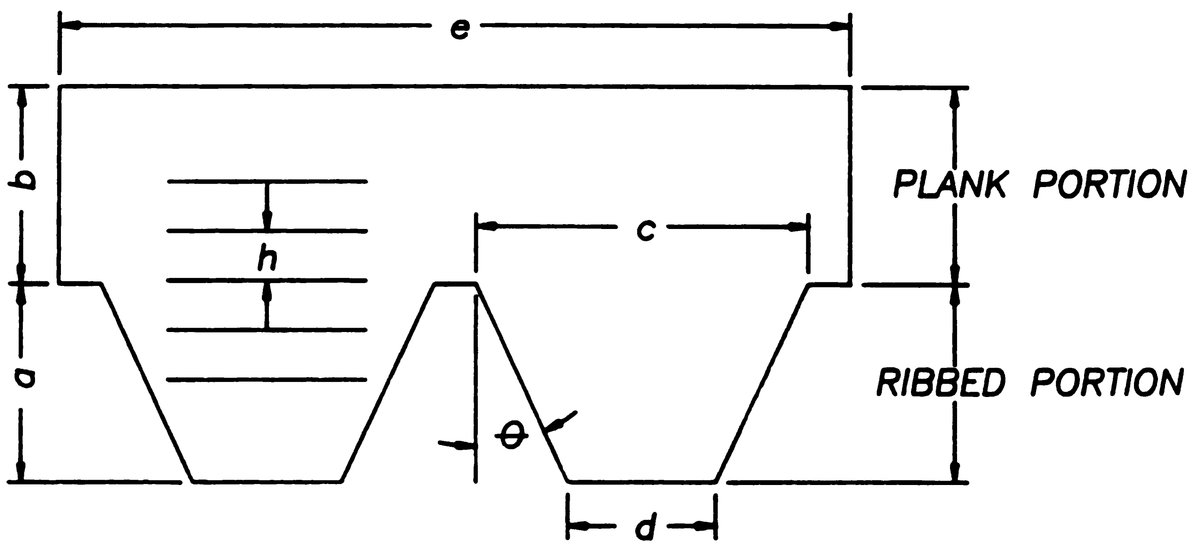

FIGURE 7. Generic dimensions of the ribbed cushions examined in the experiment.

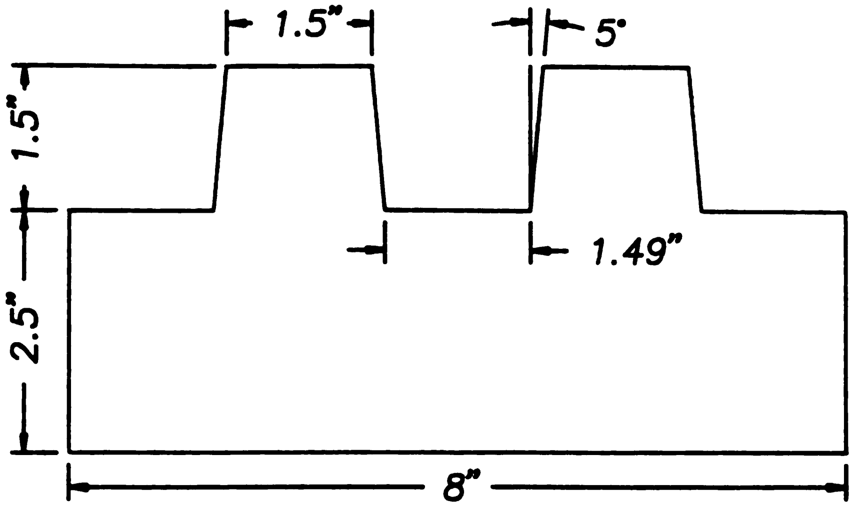

Figure 8. Rib Configuration 1.

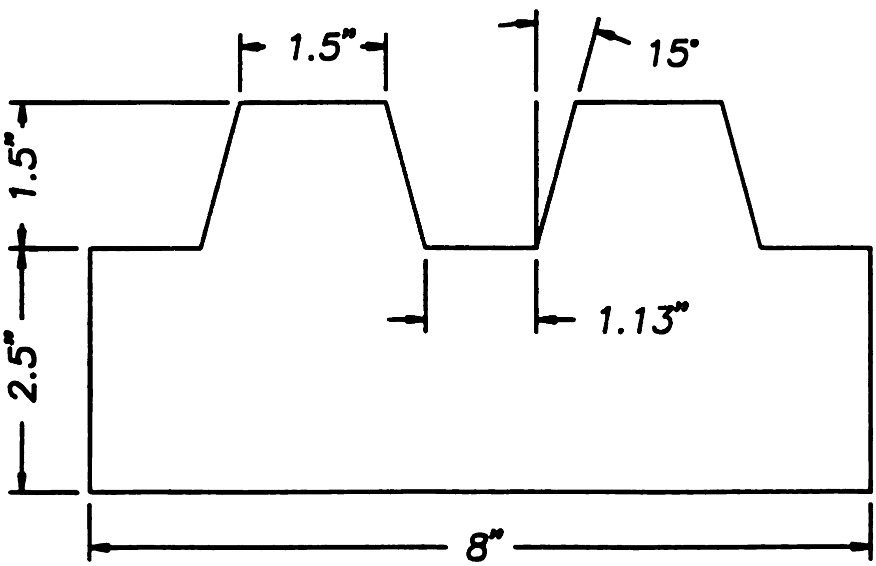

Figure 9. Rib Configuration 2.

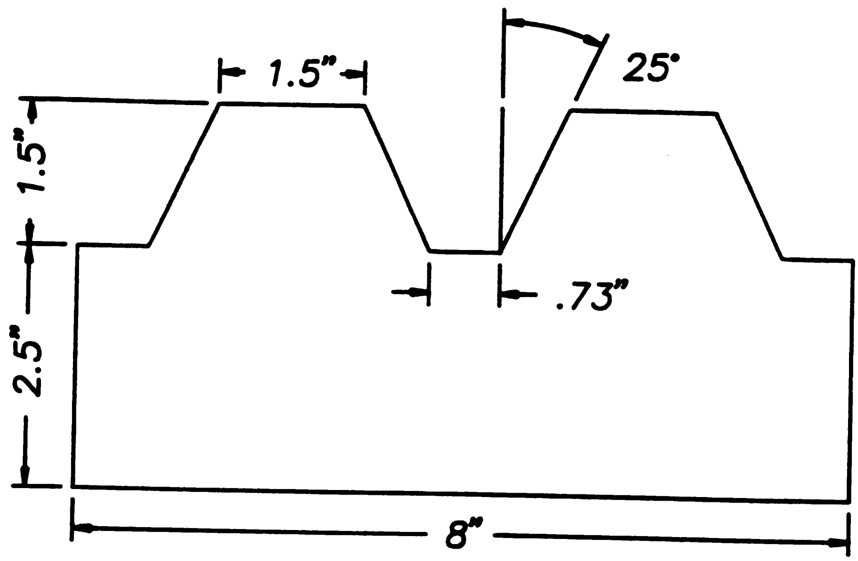

Figure 10. Rib Configuration 3.

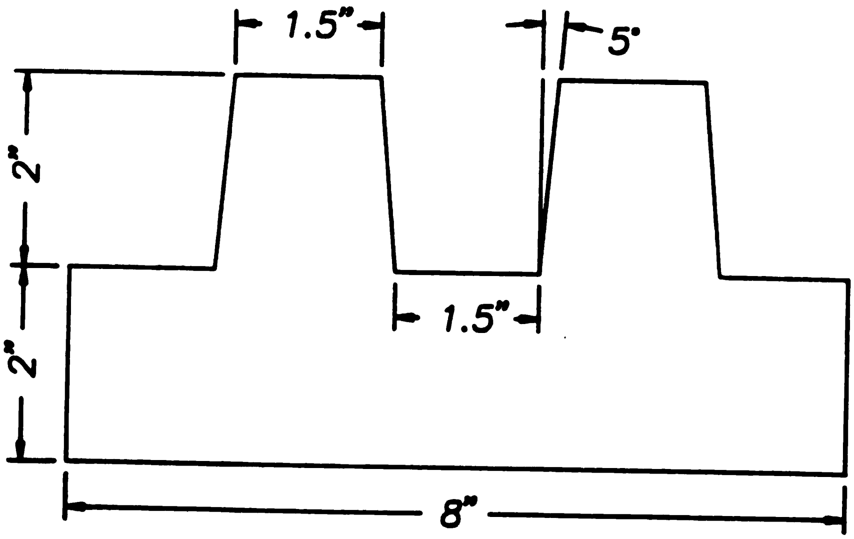

Figure 11. Rib Configuration 4.

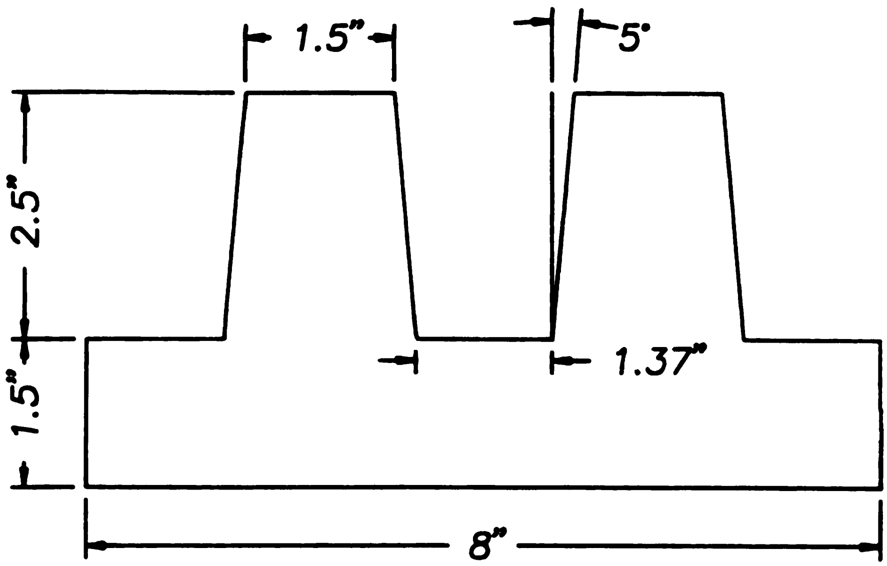

Figure 12. Rib Configuration 5.

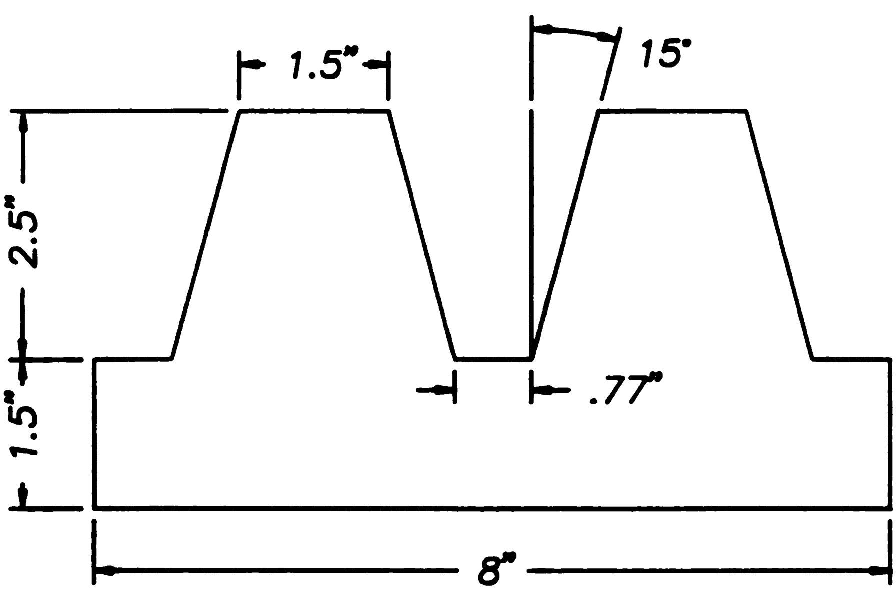

Figure 13. Rib Configuration 6.

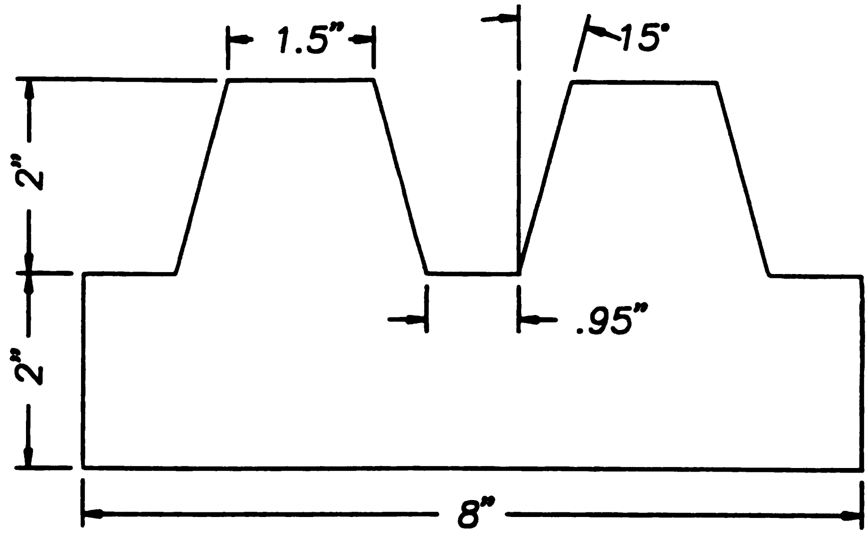

Figure 14. Rib Configuration 7.

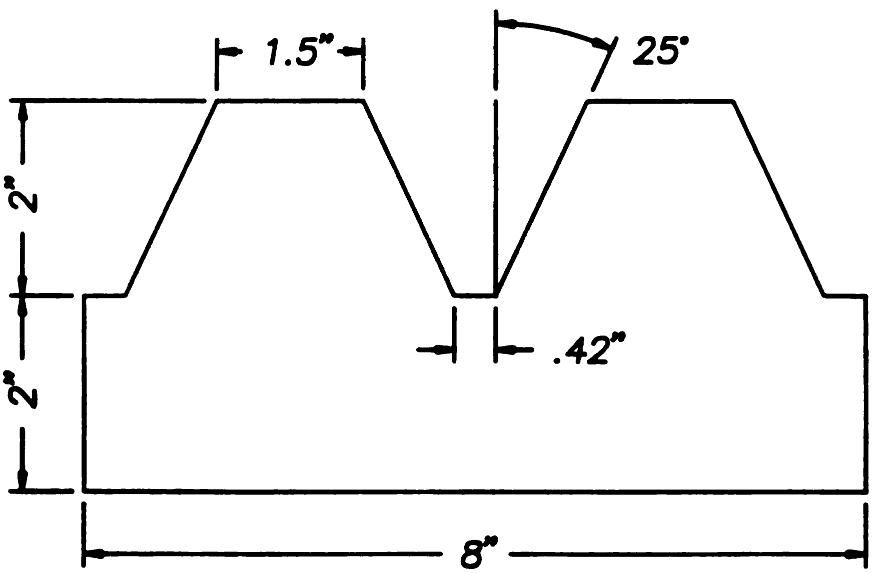

Figure 15. Rib Configuration 8.

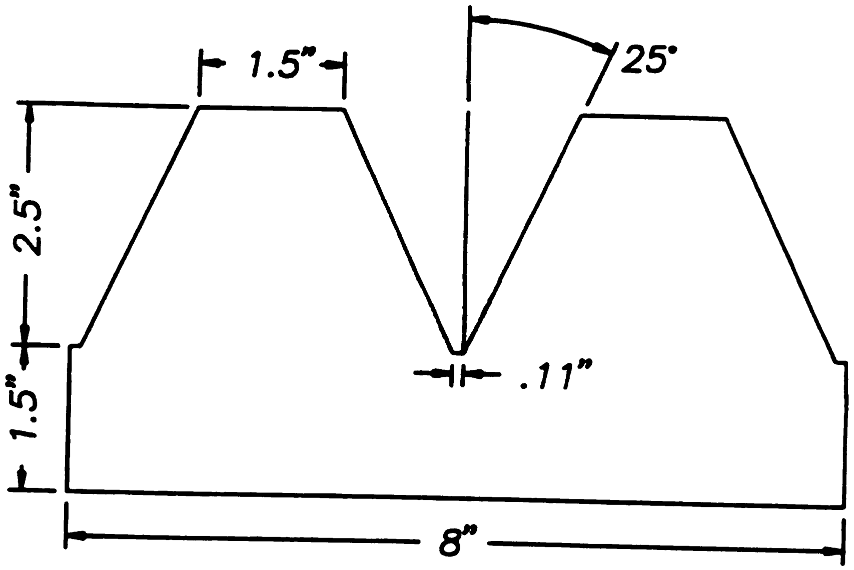

Figure 16. Rib Configuration 9.

2.3 TESTING APPARATUS

The test apparatus used was a LANSMONT MODEL 23 CUSHION TESTER. A piezoelectric accelerometer was mounted on the dropping head of the tester and the signal was carried by a shielded cable to a Kistler piezotron charge amplifier and then on to a twelve bit analog to digital card on an IBM AT compatible 80286 computer. The software used by this computer to analyze the shock pulses was Test Partner from LANSMONT CORPORATION. The shock outputs were displayed on a VGA computer monitor (See Figure 17). ASTM D1596 - 78a was used as a guideline for all testing. The drop tests onto the ribbed cushion samples were conducted as follows:

TEST PROCEDURE:

1) Hook up equipment as shown in Figure 17 and allow 10 minutes for the charge amplifier to warm up.

2) Set up the computer program to monitor and analyze the shock pulse.

3) Make sure that the guide rods are clean and have a thin film of lubrication since air friction and friction due to the sleeves contacting the guide rods will slow down the dropping head. The dropping head must be raised higher than the calculated free fall drop height.

4) Place a variety of weights on the dropping head to alter the static loading.

5) Insert a ribbed cushion sample.

6) Raise the falling platen and drop it onto the cushion.

7) Record the peak deceleration value (the computer program will display the shock pulse on the monitor).

8) Repeat steps 1 through 7 for all drop heights, static loadings, and cushion configurations.

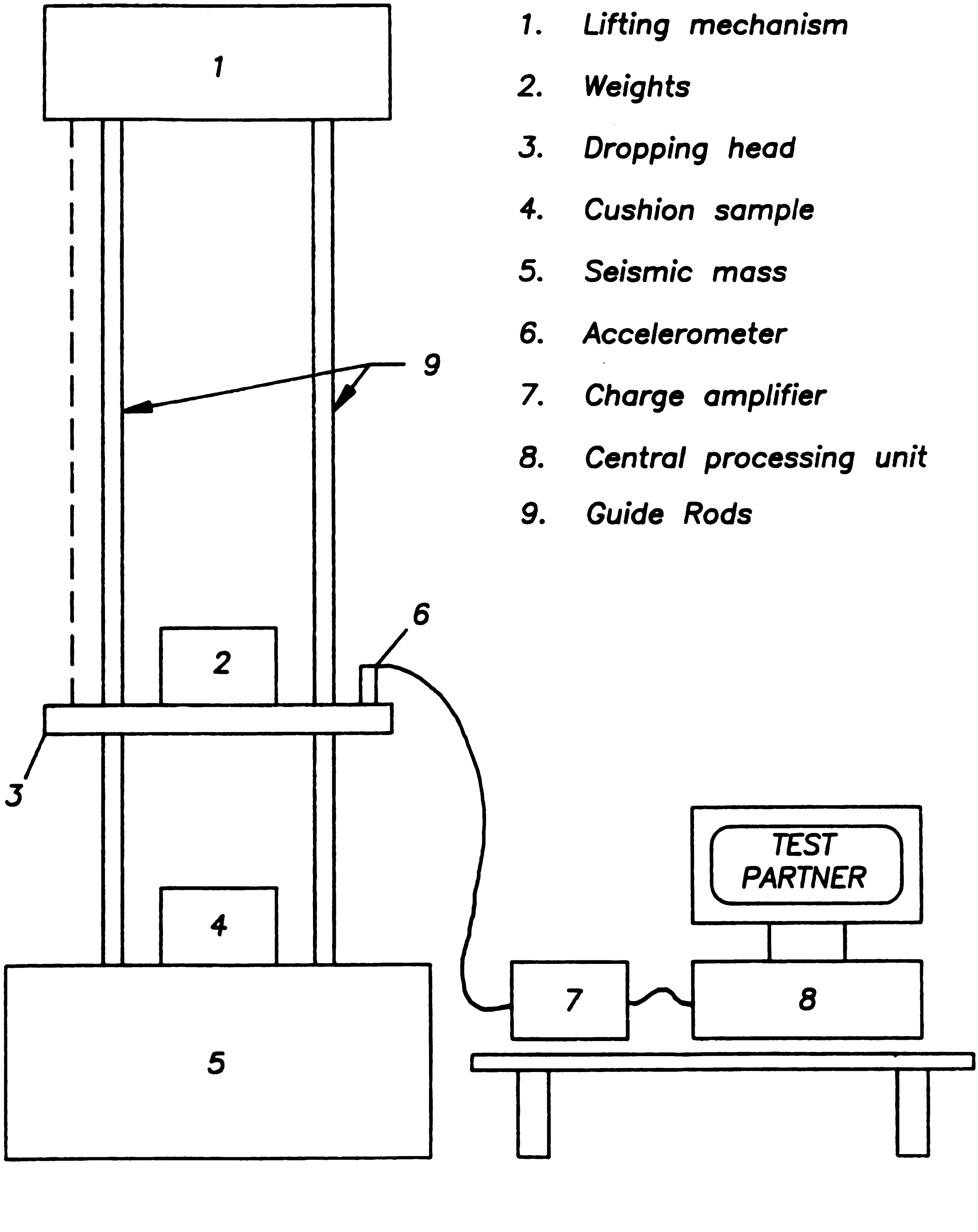

FIGURE 8. Testing apparatus and monitoring equipment.

The results of the drop tests on the ribbed cushions shown in Figures 8 through 16 are shown in Tables B1 through B9 in Appendix B. The third column of each table contains the actual peak deceleration in G's for the weight in column 2 dropped from the height in column 1 onto the configuration referred to. The remaining 7 columns deal with prediction methods and will be discussed in Chapter 3. Possible errors in the raw data will be covered next.

The greatest likely source of error associated with the technique lies in the measurement of the equivalent free fall drop height referred to in step 3. Since the actual drop height is less than the machine drop height due to friction, it must be inferred from the measured impact velocity. Two methods were used to determine the impact velocity. The first was to use a photoelectric sensor mounted just above the impact surface of the cushion which measures the amount of time (gate time) it takes for a 1/2" wide trigger blade mounted on the dropping head to pass through it. This time value can then be substituted into the following equation:

$$V = d/t + .5gt \qquad \text{Equation (3)}$$

suggested by LANSMONT CORPORATION, where:

V = impact velocity (in/sec)

d = width of the trigger blade = 1/2"

t = gate time (seconds)

The equivalent free fall drop height h corresponding to this impact velocity must be obtained from:

$$h = v^2 / 2g. \qquad \text{Equation (4)}$$

Table 3 shows the gate times and impact velocities required to produce 18", 30", and 42" free fall drops.

TABLE 3. GATE TIME, IMPACT VELOCITY & FREE FALL DROP HEIGHT

GATE TIME (Milliseconds)	IMPACT VELOCITY (inches/sec)	FREE FALL DROP HEIGHT (inches)
4.27	117.9	18
3.30	152.3	30
2.78	180.2	42

Another method used to verify the impact velocity in this experiment was to raise the dropping head to the desired equivalent free fall drop height, drop the head onto the cushion, and record the shock pulse. The Test Partner software was used to calculate the impact velocity as the area under the curve up to the peak acceleration. This procedure was repeated by adjusting the dropping head up or down until the desired impact velocity was achieved. The two methods gave similar results.

A second source for error in this experiment is the measurement of the peak deceleration. For the accelerometer used, the output voltage may be in error by as much as ± 2%. The coupler or charge amplifier which conditions the accelerometer signal, may change the signal by as much as ± 5%. The analog signal may be altered an additional 5 % in the process of passing through the signal splitter and the analog to digital conversion card in the computer. If these errors are additive, then the total error in measuring the peak deceleration may be as high as ± 12 %. Some other errors include tribo-electric noise which is caused by the cable whipping during impact, ringing noise from the test fixture after impact and electromagnetic interference from other pieces of electronic equipment in the building.

Finally, the material tested is rated at 1.9 pounds per cubic foot nominal but can vary from 1.8 PCF to 2.0 PCF depending on whether a sample is taken from the edge or the center of the plank material [Lentz, 1990]. Table 4 summarizes all of these associated errors. Based on these errors, the values for the actual G's reported in Tables B1 through B9 in Appendix B must be regarded as accurate to within ± 12% for drop heights which may be ± 6% different than those also reported.

TABLE 4. SUMMARY OF ASSOCIATED ERRORS

Drop Height:	6%
Accelerometer:	2%
Coupler:	5%
Computer Hardware	5%

CHAPTER 3

PREDICTION METHODS USING PLANK CUSHION CURVES

In this chapter, seven methods for predicting ribbed cushion performance will be presented and evaluated. These methods range from the very simple but crude to complex. A side by side comparison of the actual deceleration values obtained to the seven predicted values for each data point and configuration are shown in Appendix B. See Figures 8 - 16 for profiles of the actual cushion configurations used. The following is a detailed discussion of each method (from the simplest to most complex) and why each was considered. Since the idea is to convert a ribbed cushion into an equivalent plank cushion, each method will focus on producing a bearing area and/or thickness with which the conventional cushions curves can be used. The predicted G's referred to in Tables B1 though B9 therefore come from the cushion curves (Figure 2) with a static loading equal to the weight divided by the predicted bearing area.

Method 1: From Figure 7, the most obvious guess on the equivalent bearing area is the contact area between the product and the cushion, or "e x e" which is constant at 64 in^2. This method, although over simplified, was used in the past by packaging specialists because it was not yet well understood how ribbing affected the overall dynamic performance of the cushion. As shown in Tables B1 through B9, It does appear to work fairly well but only for the medium weights at each drop height. The trend is to overstate G for the lower weights and underestimate it at the higher weights. Because the ribbed cushion is much less stiff than one with a constant bearing area of e x e, overestimation was expected. The most probable reason for the underestimation at the higher weights is that beyond the static loading of 78.5 lbs divided by 64 in^2 (1.22 psi), Arpro® planks show a decrease in G's (see Figure 2) while the ribbed cushions are bottoming out. Based on the 'Standard error' between the predicted and the actual data, defined here to be:

$$SE = \sqrt{\frac{\sum (actual\ G's - predicted\ G's)^2}{N}} \qquad \text{Equation (5)}$$

where N = 9 is the number of predictions, this method ranked fifth in accuracy of prediction.

Method 2: This method uses the footprint of the ribbed cushion in Figure 7 to estimate the bearing area. Since there were two ribs throughout, each measuring d = 1.5" by e = 8" regardless of the configuration, the bearing area using this prediction method is constant at:

$$A = 2(d * e) \qquad \text{Equation (6)}$$

which equals 2*(1.5" X 8") = 24 in^2 for every configuration. This method ignores the substantial contribution of the plank portion when the cushion is dynamically loaded at high drop heights and high static stresses. Since the footprint area represents the other end of the spectrum for bearing area predictions, This method is expected to show the reverse trend compared to Method 1. Figures B1 through B9 confirm this. The trend now is to underestimate G for the lower weights and overstate it at the higher weights. This method ranked seventh in predicting the outcome of the experiment.

It is easily demonstrated by experiment that flipping the ribbed cushion in Figure 7 upside down so that the ribs contact the product and the plank contacts the ground does not change the shock G. This should be expected since the resistance of the cushion is affected only by the change in its thickness during compression. Based on this fact and the complimentary trends for Methods 1 and 2, it would appear that the best choice for the bearing area would be some sort of weighted average of the foot print and plank areas. The remaining methods were chosen to evaluate the various ways to weight these areas. As the results show, it is generally true that some sort of weighting procedure gives better results overall, but this is not true in all cases.

Method 3: This method uses the average of the plank and footprint areas. The bearing area is:

$$A = e(d + e/2).$$ Equation (7)

which is constant at: 8" * (1.5" + 8"/2) = 44 in^2. This method would appear to be a good "middle of the road" predictor since it does take into consideration the cross sectional change between the plank and the footprint. However, it weighs them equally regardless of the rib height b and the rib angle θ. It is therefore possible with this method to get the same prediction for G for a wide variety of rib heights and angles and also a wide variety of plank and footprint combinations so long as the average of these two is constant. For these reasons, this method is not sound even though it ranked third in predicting the outcome of this experiment.

Method 4: This method uses the area at the widest portion of the rib. From Figure 7, this area is:

$$A = 2 * (e * c)$$ Equation (8)

The reasoning here is that the force of compression is transmitted from the plank portion to the ribs through this area. Separate compression tests on these ribbed cushions show that deformation of the plank portion is greatest in the regions where the ribs meet the plank. The region in between the ribs and the outside the ribs near the edges of the plank deform very little in comparison. This interface bearing area may therefore be instrumental in determining the shock transmitted. The results in Tables B1 through B9 show that this method appears to nearly always underestimate the actual shock by about 5 G's on the average. Simply adding 5 G's to the predicted result would improve the method considerably but would be difficult to justify on physical grounds since this approach does not and cannot take into consideration variations in either the plank or the footprint. It is possible with this method to get a wide range of actual G's by varying the plank and footprint areas while keeping A = 2(e*c) constant. In spite of this short coming, this method ranked fourth in predicting the outcome of the experiment.

Method 5: This method weighs the cross sectional areas equally. An estimate of the average cross sectional area can be obtained by drawing many equally spaced horizontal lines on the cushion as in Figure 7 and averaging the areas at these sections,

$$avg\ A = \frac{\sum A's}{N} \qquad \text{Equation (9)}$$

where N is the number of sections examined (lines drawn). The true average area is obtained only in the limit as N approaches infinity. Multiplying the numerator and denominator on the right hand side of equation (9) by the uniform spacing h between the parallel lines leads to

$$avg\ A = \frac{(\sum A's) * h}{N} = \frac{\sum (A * h)}{height}$$

Equation (10)

Since N X h is the height (total thickness) of the ribbed cushion and since the area at any given section multiplied by the spacing is just the volume of material contained between two consecutive lines (one of which is at the area being examined), in the limit as N becomes large, the true average area approaches:

$$avg\ A = \frac{Total\ Cushion\ Volume}{Thickness}$$

Equation (11)

The ribbed cushions used here are made up of trapezoidal shapes. Figure 7 can be used to determine the total cushion volume V as the sum of the contributions of the two ribs and the plank portion,

$$V = 2 * \frac{(c + d)}{2} * be + ae^2$$

Equation (12)

Since the thickness is a + b, the bearing area becomes:

$$A = \frac{(c + d)}{(a + b)} * be + \frac{ae^2}{a + b}$$

Equation (13)

When used along with the weight to get the static loading, this method ranked first in predicting G. For this reason, this method will be dealt with in more detail in chapter 4.

Method 6: This method considers the cushion to be made of a linearly elastic material and applies Hooke's Law to each variable cross section of the ribbed cushion [Faupel, 1967]. When the cushion is compressed by a force **F** distributed over the top of the cushion, this same force is transmitted through every cross section. Since the area **A** changes from section to section, the stress $\sigma = F / A$ does also. From Hooke's Law, the strain ϵ (which represents the rate of change of displacement **u** with respect to elevation **x**) is just σ / E where **E** is the modulus of elasticity for the material,

$$\frac{du}{dx} = \frac{F}{EA}.$$

Equation (14)

The total compression of the cushion is therefore:

$$u = \frac{F}{E}\int_0^t \frac{dx}{A}$$

Equation (15)

In the case of an equivalent plank cushion where the area is constant at A_c, the above expression yields,

$$u = \frac{Ft}{EA_c}.$$

Equation (16)

Forcing the ribbed and the plank cushions to be equivalent in producing for a given force **F** the same compression u, requires that the bearing area be:

$$A_c = \frac{t}{\int_0^t \frac{dx}{A}} \qquad \text{Equation (17)}$$

As with method 5, the bearing area may be approximated by drawing N equally spaced horizontal lines on the ribbed cushion and obtaining the area A_1, A_2, A_3 ... A_N at these sections. If the spacing between lines is constant at h, then:

$$A_c = \frac{Nh}{\frac{h}{A_1} + \frac{h}{A_2} \cdots + \frac{h}{A_N}} = \frac{N}{\frac{1}{A_1} + \frac{1}{A_2} \cdots + \frac{1}{A_N}} \qquad \text{Equation (18)}$$

The exact value can be obtained only by integration. Again, referring to Figure 7, since the cushion is made up of two parts, the rib portion and the plank portion, the integral

$$I = \int_0^t \frac{dx}{A} \qquad \text{Equation (19)}$$

is the sum of the separate integrals over the plank and rib portion,

$$I_{plank} = \int_0^a \frac{dx}{e} * e = \frac{a}{e^2} \qquad \text{Equation (20)}$$

For the two ribs,

$$I_{ribs} = \int_0^b \frac{dx}{2[e*c + (e*d - e*c) * (x/b)]} \qquad \text{Equation (21)}$$

$$I_{ribs} = \frac{b}{2*e(c - d)} \ln \frac{c}{d} \qquad \text{Equation (22)}$$

Combining these two, the bearing area becomes:

$$A = \frac{(a + b) * e}{\frac{a}{w} + \frac{b}{2(c - d)} \ln \frac{c}{d}} \qquad \text{Equation (23)}$$

This method works well for "average" conditions and ranked second in predicting the outcome of this experiment. This method is suspect however because the material is unlikely to be linear which is probably why it fails to predict G at extreme static loadings and drop heights.

Method 7: Up to now, all of the prediction methods have been based on converting a ribbed cushion into an equivalent plank cushion which has the same thickness as the ribbed cushion but has a different bearing area. This method takes the area of the equivalent plank cushion to be the same as the plank area of the ribbed cushion and chooses the thickness so that the volumes of the ribbed and equivalent plank cushions are the same. This is the compliment of the average area method (Method 5). Suppose for example that a ribbed cushion consists of a 1" thick plank portion measuring 8" X 8" with 3" thick ribs where the total rib volume is 64 cubic inches. The total cushion volume is therefore 8 X 8 X 1 + 64 = 128 cubic inches. With this method, the bearing area would be 8" X 8" = 64 in^2 and the equivalent thickness would be 128 in^3 / 64 in^2 = 2 inches. Note that with Method 5, the thickness is 1" + 3" = 4" but the equivalent bearing area is 128 in^3 / 4 in = 32 in^2. This method works rather well at medium to high drop heights and static loadings as expected because the plank area is now being accounted for, but fails to predict well at lower drop heights and static loadings. This method ranked sixth in predicting the outcome of the experiment.

CHAPTER 4

4.1 DISCUSSION AND CONCLUSION

Since Method 5 ranked #1 in predicting G compared to the six other methods presented, the reasons for its performance will be investigated here. Up to this point, we have referred to this method as the "true average area" method since it equally weighs each cross sectional area from bottom to top. In essence, this method makes a plank cushion with the same thickness out of the same amount of material which reduces the bearing area in the process. Keeping the thickness the same ensures that the travel distance allotted to the decelerating mass in coming to rest during impact remains unchanged. Keeping the volume the same ensures that the material which actually absorbs the energy from the impact is still there in the same quantity. More specifically, when the air that is trapped inside a closed cell cushion is compressed, it is the total air <u>volume</u> which determines the resistance to compression. The proof of this is in the Gas Law: [Benning, 1969],

$$pV = nRT: \qquad \text{Equation (24)}$$

Where p is the absolute pressure of the air inside the cells, V is the total air volume, n is the number of moles occupying this volume, T is the absolute temperature, and R is the universal gas constant, $R = 45.61$ ml - atm / mole-°R. During the dynamic compression of a closed cell foam, the temperature of the air trapped in the cells remains essentially constant [Burgess, 1988]. Since the cells are closed, the quantity of air (n moles) also remains constant. The Gas Law therefore states that the product of the pressure and volume remains constant at p_oV_o ,

$$pV = p_oV_o \qquad \text{Equation (25)}$$

Where p_o = 1 atmosphere is the cell air pressure before compression and $V_o = At$ where A is the bearing area and t is the thickness. Equation (25) states that as the cushion is compressed, the volume decreases and the air pressure inside the cells increases. Since the resistance to compression is just the air pressure multiplied by the bearing area, the resistance therefore increases in proportion to the decrease in volume. It can be shown [Burgess, 1988] that the cushion curves for flat planks may be derived on the basis of this air compression model. For these reasons, it is reasonable to expect now that it is cushion volume which determines G and this is the heart of Method 5. In light of these facts, we now should view this model as the Equivalent Volume Method.

The total standard error for each method was obtained by using all of the predicted G versus actual G data for all of the cushion configurations (Tables B1 though B9) for the particular method in question in Equation 5. In each case then, N = 81. The results are shown in Table B10. The total standard error for the Equivalent Volume Method was lowest at 4.8 G's. Total experimental measurement error on G was ± 12 % from Table 4. Also, the cushion curves are reported for a given nominal density, which is 1.9 pounds per cubic foot for

Arpro® 3319. However, the density of the samples tested varied from 1.8 PCF to 2.0 PCF which is normal according to ARCO CHEMICAL'S Analytical Services people [Becker, 1990]. This difference in density can change the actual deceleration values obtained by ± 5 G's from the values reported in the cushion curves. For these reasons, an analysis was carried out to see how much of the Standard Error value of 4.8 G's for the Equivalent Volume Method could be explained by experimental error. For example, if the actual and predicted G's are 25 G and 35 G respectively, then the actual G could have been 25 + 12 % = 28 G and the predicted G could have been 35 - 5 = 30 G. The remaining discrepancy of 30 - 28 = 2 G can only be attributed to the method error. The computer program in Appendix C, varies the actual G columns of Tables B1 through B9 up or down by as much as ± 5 G's and the predicted G's from the Equivalent Volume (column 5) up or down by as much as ± 12 %, whichever way reduces the discrepancy. In line 10 of the program, the actual and the predicted G's for all 81 of the data points in Tables B1 through B9 are stored in the dimensions GA and GP respectively. Lines 20 through 40 read the data into these dimensions. Lines 50 through 120 reduce the difference between the actual and predicted G's by the maximum amount allowed (± 12 % on actual G, ± 5 G on predicted G) and record the remaining difference in the dimension DIFF. Lines 130 to 170 calculate the Standard Error using Equation (5). The reduced standard error taking into account these errors becomes 0.09 G's. Therefore, all of the difference between actual and predicted actual and predicted G's can be explained by measurement error except for 0.09 G's which must be associated with the method.

Based on this result and the simplicity of the method, the Equivalent Volume Method should be regarded as the "method of choice" when trying to determine the bearing area for a cushion design even though it is not a perfect model. It is fairly simple to use and should give engineers a useful tool to help cut down the amount of time needed for a ribbed cushion design.

4.2 RECOMMENDATIONS FOR FUTURE RESEARCH

The amount of deflection that the cushion experiences during impact may help to explain why the predicted results were not very close to correct for the extremes of static loading and drop height. A similar experiment may be performed that would include a high speed video camera that could observe the amount of deformation in the various components (plank and rib portions) of the cushion. It is most probable that in light static loading and low drop heights, the ribbed portion of the cushion was absorbing most of the shock. Therefore, the method was overestimating the contribution of the plank portion of the cushion to the total bearing area. In contrast, for higher static loading and greater drop heights, the plank portion of the cushion was absorbing more of the shock and therefore the method was underestimating the contribution of the plank portion. A high speed video camera could capture these events and allow for closer scrutiny that in turn could help improve the model.

Also, due to the size constraint of the cushion tester used, only cushions up to 8" x 8" could be tested. The rib angle of the cushion could therefore only be a maximum of 25 degrees when the plank thickness was 1.5" and the number of ribs was 2. Consequently, the cushion configurations were relatively similar in shape. This may account for the good performance of the model. A cushion tester with a larger dropping surface area could allow for the study of many ribs and larger rib angles to see if the method works just as well with more variance of the cushion parameters.

APPENDIX A

RIBBED CUSHION SURVEY

APPENDIX A: RIBBED CUSHION SURVEY

Dear Packaging Specialist:

I am a graduate student at Michigan State University in the school of Packaging and I am working on a thesis involving ribbed cushions. I would appreciate it very much if you would take a couple of minutes of you time to fill out this survey and return if to me at your convenience. Thank you very much for your time.

Sincerely,

Gary C. Granthen

Gary C. Granthen

I. Your Job Title

A) Packaging Engineer
B) Packaging Supplier
C) Other (Please specify)

II. Main Duties Performed.

A) Designing packages for your company.
B) Designing and/or selling packages to other companies.
C) Other (Please specify).

III. Do you design and/or use ribbed cushions? (Closed cell)

A) Yes
B) No

IV. If your answer to III is yes, place in order of importance the following reasons why you use them (1 = most important reason).

__ Ease of hand fabrication for short term production runs.
__ Ease of molding for long term production runs.
__ Reducing G-levels for a high product surface area scenario.
__ Lower cost than plank cushion for the same performance.
__ Better performance with less material.
__ Company requires you to.
__ Status Quo.
__ Other (Please specify). ______________________________

V. If your answer to III. is no, please state why not in the space below.

____

____

APPENDIX B

TABLES B1 THROUGH B10

APPENDIX B. TABLES B1 – B10

TABLE B1. ACTUAL AND PREDICTED PEAK DECELERATION VALUES FOR CONFIGURATION 1 (IN G'S).

DROP HEIGHT	WEIGHT (POUNDS)	ACTUAL G'S	1	2	3	4	5	6	7
18"	41.4	25.5	40.2	18.3	29.6	20.3	32.9	28.0	41.8
18"	72.3	21.0	25.2	11.9	18.8	14.7	20.5	18.2	27.0
18"	103.3	19.0	19.1	23.5	15.7	9.9	16.7	15.0	20.8
30"	41.4	33.5	42.8	24.0	33.1	26.3	35.8	32.0	45.4
30"	72.3	29.3	30.0	20.0	24.7	19.9	26.5	23.8	32.8
30"	103.3	28.5	25.0	39.7	20.4	23.2	21.6	20.0	28.9
42"	41.4	42.8	48.8	29.3	37.5	30.2	40.8	36.0	53.0
42"	72.3	37.5	33.5	30.1	29.5	29.0	30.3	29.2	39.3
42"	103.3	39.0	29.6	76.2	29.0	40.4	29.0	29.0	37.1
STANDARD ERROR (G'S)			7.3	31.6	5.9	7.8	5.6	5.6	8.0

BEARING AREA PREDICTION METHOD NUMBER	AREA (IN^2)
1. PLANK AREA = e^2	64.0
2. FOOTPRINT AREA = 2de	24.0
3. AVERAGE OF PLANK AND FOOTPRINT AREAS = e(d + e/2)	44.0
4. TOP OF RIB AREA = 2ec	26.1
5. TRUE AVERAGE AREA = e * [(e + a) + b + (c + d)] / (a + b)	49.8
6. HOOKE'S LAW AREA = (a + b) * e / [(a/e) + b/2 * (c − d) ln(c/d)]	41.4
7. EQUIVALENT THICKNESS AREA = e^2 ; T = (c + d) * b * (e/64) + a	64.0

APPENDIX B (cont,d.)

TABLE B2. ACTUAL AND PREDICTED PEAK DECELERATION VALUES FOR CONFIGURATION 2 (IN G'S).

DROP HEIGHT	WEIGHT (POUNDS)	ACTUAL G'S	1	2	3	4	5	6	7
18"	44.9	27.0	37.8	17.6	27.5	23.6	31.5	28.0	39.2
18"	78.5	21.8	23.4	10.3	18.0	16.5	19.7	18.2	25.0
18"	112.3	20.0	18.1	44.3	14.8	11.7	16.3	15.0	19.7
30"	44.9	33.5	40.2	22.9	31.7	28.9	34.7	32.0	42.6
30"	78.5	29.0	28.8	20.6	23.5	21.2	25.7	23.8	31.4
30"	112.3	28.5	23.8	62.7	19.9	20.1	21.0	20.0	27.7
42"	44.9	41.0	46.0	29.1	35.6	32.3	39.4	36.0	49.9
42"	78.5	35.5	32.2	32.2	29.2	29.0	29.9	29.2	37.6
42"	112.3	36.3	29.2	112.9	29.0	30.3	29.0	29.0	36.3
STANDARD ERROR (G'S)			5.5	31.0	5.5	6.8	4.6	4.6	6.1

BEARING AREA PREDICTION METHOD NUMBER	AREA (IN ^{2})
1. PLANK AREA $= e^2$	64.0
2. FOOTPRINT AREA $= 2de$	24.0
3. AVERAGE OF PLANK AND FOOTPRINT AREAS $= e(d + e/2)$	44.0
4. TOP OF RIB AREA $= 2ec$	30.4
5. TRUE AVERAGE AREA $= e * [(e + a) + b + (c + d)] / (a + b)$	51.4
6. HOOKE'S LAW AREA $= (a + b) * e / [(a/e) + b/2 * (c - d) \ln(c/d)]$	44.9
7. EQUIVALENT THICKNESS AREA $= e^2$; $T = (c + d) * b * (e/64) + a$	64.0

APPENDIX B (cont,d.)

TABLE B3. ACTUAL AND PREDICTED PEAK DECELERATION VALUES FOR CONFIGURATION 3 (IN G'S).

DROP HEIGHT	WEIGHT (POUNDS)	ACTUAL G'S	1	2	3	4	5	6	7
18"	48.1	28.0	35.8	17.0	25.9	27.1	30.6	28.0	37.0
18"	84.1	20.0	22.1	9.6	17.4	17.8	19.3	18.2	23.5
18"	120.2	19.0	17.5	68.9	13.7	14.5	16.0	15.0	18.8
30"	48.1	34.5	38.3	22.0	30.5	31.4	33.9	32.0	40.3
30"	84.1	28.0	27.8	21.8	22.6	23.3	25.3	23.8	30.2
30"	120.2	28.5	22.8	91.5	19.8	19.9	20.7	20.0	26.5
42"	48.1	40.5	43.8	29.0	34.2	35.2	38.5	36.0	47.3
42"	84.1	35.3	31.3	36.2	29.0	29.1	29.7	29.2	36.2
42"	120.2	37.8	29.1	151.2	29.2	29.0	29.0	29.0	35.5
STANDARD ERROR (G'S)			4.9	31.0	5.9	5.5	4.7	4.7	4.6

BEARING AREA PREDICTION METHOD NUMBER	AREA (IN^2)
1. PLANK AREA = e^2	64.0
2. FOOTPRINT AREA = $2de$	24.0
3. AVERAGE OF PLANK AND FOOTPRINT AREAS = $e(d + e/2)$	44.0
4. TOP OF RIB AREA = $2ec$	35.1
5. TRUE AVERAGE AREA = $e * [(e + a) + b + (c + d)] / (a + b)$	53.2
6. HOOKE'S LAW AREA = $(a + b) * e / [(a/e) + b/2 * (c - d) \ln(c/d)]$	48.1
7. EQUIVALENT THICKNESS AREA = e^2 ; $T = (c + d) * b * (e/64) + a$	64.0

APPENDIX B (cont,d.)

TABLE B4. ACTUAL AND PREDICTED PEAK DECELERATION VALUES FOR CONFIGURATION 4 (IN G'S).

DROP HEIGHT	WEIGHT (POUNDS)	ACTUAL G'S	1	2	3	4	5	6	7
18"	37.6	25.5	43.1	19.4	32.1	22.7	33.0	28.0	45.3
18"	65.8	17.3	27.3	13.7	20.0	16.2	20.5	18.2	29.7
18"	94.2	18.0	20.3	12.6	16.5	10.8	16.7	15.0	22.6
30"	37.6	32.0	46.0	25.4	35.1	28.3	35.8	32.0	49.5
30"	65.8	28.0	31.5	19.8	26.0	20.8	26.5	23.8	35.0
30"	94.2	28.0	26.3	27.3	21.2	20.4	21.6	20.0	30.8
42"	37.6	36.5	52.1	29.7	40.0	31.7	40.9	36.0	57.3
42"	65.8	35.5	35.4	29.2	30.0	29.0	30.3	29.2	42.5
42"	94.2	37.0	30.1	51.0	29.0	31.3	29.0	29.0	39.3
STANDARD ERROR (G'S)			10.1	29.5	4.9	5.6	5.1	5.1	12.5

BEARING AREA PREDICTION METHOD NUMBER	AREA (IN^2)
1. PLANK AREA = e^2	64.0
2. FOOTPRINT AREA = $2de$	24.0
3. AVERAGE OF PLANK AND FOOTPRINT AREAS = $e(d + e/2)$	44.0
4. TOP OF RIB AREA = $2ec$	26.8
5. TRUE AVERAGE AREA = $e * [(e + a) + b + (c + d)] / (a + b)$	45.4
6. HOOKE'S LAW AREA = $(a + b) * e / [(a/e) + b/2 * (c - d) \ln(c/d)]$	37.7
7. EQUIVALENT THICKNESS AREA = e^2 ; $T = (c + d) * b * (e/64) + a$	64.0

APPENDIX B (cont,d.)

TABLE B5. ACTUAL AND PREDICTED PEAK DECELERATION VALUES FOR CONFIGURATION 5 (IN G'S).

DROP HEIGHT	WEIGHT (POUNDS)	ACTUAL G'S	1	2	3	4	5	6	7
18"	42.4	36.8	39.5	18.1	28.9	27.3	31.4	28.1	41.3
18"	74.5	19.0	24.5	11.3	18.5	17.8	19.6	18.1	26.5
18"	106.2	18.0	18.7	29.3	15.4	14.6	16.3	15.0	20.6
30"	42.4	32.5	42.0	23.7	32.7	31.5	34.5	32.0	44.9
30"	74.5	27.0	29.6	20.2	24.3	23.3	25.6	23.8	32.7
30"	106.2	30.0	24.6	46.0	20.2	19.9	20.9	20.0	29.1
42"	42.4	36.5	47.9	29.2	36.9	35.3	39.2	36.1	52.6
42"	74.5	35.0	33.0	30.6	29.3	29.1	29.8	29.2	39.5
42"	106.2	39.0	29.4	87.1	29.0	29.0	29.0	29.0	37.9
STANDARD ERROR (G'S)			6.6	31.3	5.8	6.3	5.3	5.3	7.8

BEARING AREA PREDICTION METHOD NUMBER	AREA (IN^2)
1. PLANK AREA = e^2	64.0
2. FOOTPRINT AREA = $2de$	24.0
3. AVERAGE OF PLANK AND FOOTPRINT AREAS = $e(d + e/2)$	44.0
4. TOP OF RIB AREA = $2ec$	32.5
5. TRUE AVERAGE AREA = $e * [(e + a) + b + (c + d)] / (a + b)$	48.3
6. HOOKE'S LAW AREA = $(a + b) * e / [(a/e) + b/2 * (c - d) \ln(c/d)]$	42.5
7. EQUIVALENT THICKNESS AREA = e^2 ; $T = (c + d) * b * (e/64) + a$	64.0

APPENDIX B (cont,d.)

TABLE B6. ACTUAL AND PREDICTED PEAK DECELERATION VALUES FOR CONFIGURATION 6 (IN G'S).

DROP HEIGHT	WEIGHT (POUNDS)	ACTUAL G'S	1	2	3	4	5	6	7
18"	46.8	28.5	36.6	17.2	26.5	31.7	30.4	28.0	38.0
18"	82.0	20.8	22.6	9.7	17.6	19.8	19.2	18.2	24.2
18"	117.2	16.5	17.7	59.5	14.1	16.3	16.0	15.0	19.2
30"	46.8	32.3	39.0	22.3	31.0	34.8	33.8	32.0	41.4
30"	82.0	25.5	28.2	21.3	22.9	25.8	25.1	23.8	30.8
30"	117.2	26.5	23.2	80.2	19.8	21.0	20.6	20.0	27.3
42"	46.8	37.0	44.6	29.0	34.7	39.5	38.3	36.0	48.6
42"	82.0	33.5	31.6	34.4	29.1	29.9	29.6	29.2	37.1
42"	117.2	38.0	29.1	136.9	29.1	29.0	29.0	29.0	36.4
STANDARD ERROR (G'S)			5.5	29.5	4.4	4.1	4.0	4.0	6.4

BEARING AREA PREDICTION METHOD NUMBER	AREA (IN^2)
1. PLANK AREA = e^2	64.0
2. FOOTPRINT AREA = 2de	24.0
3. AVERAGE OF PLANK AND FOOTPRINT AREAS = e(d + e/2)	44.0
4. TOP OF RIB AREA = 2ec	26.1
5. TRUE AVERAGE AREA = e * [(e + a) + b + (c + d)] / (a + b)	51.5
6. HOOKE'S LAW AREA = (a + b) * e / [(a/e) + b/2 * (c − d) ln(c/d)]	46.8
7. EQUIVALENT THICKNESS AREA = e^2 ; T = (c + d) * b * (e/64) + a	64.0

APPENDIX B (cont,d.)

TABLE B7. ACTUAL AND PREDICTED PEAK DECELERATION VALUES FOR CONFIGURATION 7 (IN G'S).

DROP HEIGHT	WEIGHT (POUNDS)	ACTUAL G'S	1	2	3	4	5	6	7
18"	34.8	26.5	45.5	20.5	34.3	25.3	32.4	28.0	48.2
18"	61.0	19.0	29.2	14.8	21.2	17.1	20.2	18.2	32.0
18"	87.0	17.5	21.5	9.7	17.1	13.3	16.6	15.0	24.5
30"	34.8	33.0	48.8	26.5	37.0	30.1	35.4	32.0	53.1
30"	61.0	25.0	32.9	19.9	27.1	22.2	26.2	23.8	37.1
30"	87.0	26.3	27.4	22.8	22.1	19.8	21.3	20.0	32.5
42"	34.8	36.3	54.9	30.3	42.2	33.7	40.3	36.0	61.0
42"	61.0	34.0	37.1	29.0	30.7	29.0	30.1	29.2	45.4
42"	87.0	38.5	30.9	39.2	29.0	29.3	29.0	29.0	41.5
STANDARD ERROR (G'S)			11.6	29.3	5.2	4.7	4.6	4.8	15.0

BEARING AREA PREDICTION METHOD NUMBER	AREA (IN ^{2})
1. PLANK AREA = e^2	64.0
2. FOOTPRINT AREA = 2de	24.0
3. AVERAGE OF PLANK AND FOOTPRINT AREAS = $e(d + e/2)$	44.0
4. TOP OF RIB AREA = 2ec	27.5
5. TRUE AVERAGE AREA = $e * [(e + a) + b + (c + d)] / (a + b)$	41.2
6. HOOKE'S LAW AREA = $(a + b) * e / [(a/e) + b/2 * (c - d) \ln(c/d)]$	34.8
7. EQUIVALENT THICKNESS AREA = e^2; $T = (c + d) * b * (e/64) + a$	64.0

APPENDIX B (cont,d.)

TABLE B8. ACTUAL AND PREDICTED PEAK DECELERATION VALUES FOR CONFIGURATION 8 (IN G'S).

DROP HEIGHT	WEIGHT (POUNDS)	ACTUAL G'S	1	2	3	4	5	6	7
18"	40.8	28.5	40.6	18.5	29.9	30.8	30.9	28.0	42.7
18"	71.6	20.0	25.4	12.1	18.9	19.3	19.4	18.1	27.7
18"	102.2	18.5	19.2	21.8	15.8	16.1	16.1	15.0	21.4
30"	40.8	33.0	43.2	24.2	33.4	34.0	34.2	32.0	46.7
30"	71.6	28.0	30.2	20.0	24.8	25.3	25.4	23.8	33.7
30"	102.2	26.3	25.1	37.7	20.4	20.7	20.8	20.0	30.1
42"	40.8	37.5	49.2	29.3	37.8	38.6	38.8	36.0	54.6
42"	71.6	34.0	33.7	29.9	29.5	29.7	29.7	29.2	41.1
42"	102.2	39.0	29.6	72.6	29.0	29.0	29.0	29.0	39.2
STANDARD ERROR (G'S)			7.5	30.2	4.4	4.4	4.4	4.4	9.7

BEARING AREA PREDICTION METHOD NUMBER	AREA (IN^2)
1. PLANK AREA = e^2	64.0
2. FOOTPRINT AREA = 2de	24.0
3. AVERAGE OF PLANK AND FOOTPRINT AREAS = e(d + e/2)	44.0
4. TOP OF RIB AREA = 2ec	34.7
5. TRUE AVERAGE AREA = e * [(e + a) + b + (c + d)] / (a + b)	45.7
6. HOOKE'S LAW AREA = (a + b) * e / [(a/e) + b/2 * (c − d) ln(c/d)]	40.9
7. EQUIVALENT THICKNESS AREA = e^2 ; T = (c + d) * b * (e/64) + a	64.0

APPENDIX B (cont,d.)

TABLE B9. ACTUAL AND PREDICTED PEAK DECELERATION VALUES FOR CONFIGURATION 9 (IN G'S).

DROP HEIGHT	WEIGHT (POUNDS)	ACTUAL G'S	1	2	3	4	5	6	7
18"	46.4	29.0	36.8	17.3	26.7	35.6	30.2	28.0	38.3
18"	81.2	21.5	22.8	9.8	17.7	22.0	19.1	18.2	24.5
18"	115.8	20.0	17.8	55.1	14.3	17.5	15.9	15.0	19.4
30"	46.4	36.0	39.3	22.4	31.1	38.1	33.7	32.0	41.8
30"	81.2	28.5	28.3	21.1	23.1	27.7	25.1	23.8	31.1
30"	115.8	27.5	23.3	75.0	19.8	22.8	20.6	20.0	27.7
42"	46.4	39.5	44.9	29.0	34.9	43.6	38.1	36.0	49.1
42"	81.2	36.0	31.8	33.8	29.1	31.2	29.6	29.2	37.6
42"	115.8	39.0	29.1	130.1	29.1	29.1	29.0	29.0	36.8
STANDARD ERROR (G'S)			5.2	31.5	6.1	4.9	5.1	5.1	5.2

BEARING AREA PREDICTION METHOD NUMBER	AREA (IN ^{2})
1. PLANK AREA = e^2	64.0
2. FOOTPRINT AREA = 2de	24.0
3. AVERAGE OF PLANK AND FOOTPRINT AREAS = $e(d + e/2)$	44.0
4. TOP OF RIB AREA = 2ec	42.7
5. TRUE AVERAGE AREA = $e * [(e + a) + b + (c + d)] / (a + b)$	50.6
6. HOOKE'S LAW AREA = $(a + b) * e / [(a/e) + b/2 * (c - d) \ln(c/d)]$	46.4
7. EQUIVALENT THICKNESS AREA = e^2 ; $T = (c + d) * b * (e/64) + a$	64.0

APPENDIX B (cont,d.)

TABLE B10. TOTAL STANDARD ERROR FOR EACH METHOD (IN G'S).

PREDICTION METHOD #	1	2	3	4	5	6	7
STANDARD ERROR (G'S)	7.5	30.6	5.4	5.7	4.8	5.2	9.0

BEARING AREA PREDICTION METHOD NUMBER

1. PLANK AREA = e^2
2. FOOTPRINT AREA = $2de$
3. AVERAGE OF PLANK AND FOOTPRINT AREAS = $e(d + e/2)$
4. TOP OF RIB AREA = $2ec$
5. TRUE AVERAGE AREA = $e * [(e + a) + b + (c + d)] / (a + b)$
6. HOOKE'S LAW AREA = $(a + b) * e / [(a/e) + b/2 * (c - d) \ln(c/d)]$
7. EQUIVALENT THICKNESS AREA = e^2 ; $T = (c + d) * b * (e/64) + a$

APPENDIX C

COMPUTER PROGRAM

APPENDIX C

COMPUTER PROGRAM TO REMOVE EXPERIMENTAL ERROR

```
05    REM:  ACTUAL G'S, PREDICTED G'S, AND DIFFERENCE
10    DIM GA(81), GP(81), DIFF(81)
20    FOR I=1 TO 81
30    READ GA(I), GP(I)
40    NEXT I
50    FOR I=1 TO 81
60    DIFF(I)=ABS(GA(I)-GP(I))
70    TOL=.12*GA(I) + 5
80    IF DIFF(I)>TOL THEN 110
90    DIFF(I) = 0
100   GOTO 120
110   DIFF(I)=DIFF(I)-TOL
120   NEXT I
130   SUM=0
140   FOR I=1 TO 81
150   SUM = SUM + DIFF(I)^2
160   NEXT I
170   STDERR=SQR(SUM/81)
180   PRINT "STDERR =       G'S"
190   PRINT STDERR
200   END
RUN
STDERR = .09 G'S
```

LIST OF REFERENCES

LIST OF REFERENCES

1. American Society for Testing and Materials, "Standard Test Method for Shock Absorbing Characteristics of Package Cushioning Materials", ASTM Method D 1596 - 78a, (Reapproved, 1983).

2. American Society for Testing and Materials, "Mechanical-Shock Fragility Of Products Using Shock Machines", ASTM Method D 3332 - 88.

3. Becker, W. P., Arco Chemical Analytical Service Engineer, personal communication, November, 1990.

4. Benning, C. J., "Plastic Foams; The Physics and Chemistry of Product Performance and Process Technology." Volume II. "Structure Properties and Applications", New York, Wiley-Interscience, 1969.

5. Burgess, G. J., "Some Thermodynamic Observations on the Mechanical Properties of Cushions", Journal Of Cellular Plastics, January 1988.

6. Chen, G. K., "The Effect of Ribbing on Shock Transmission Through Expanded PolyStyrene Cushion Material", Michigan State University, 1986.

7. Faupel, J. H., "Engineering Design", John Wiley and Sons, New York, 1967.

8. Hanlon, J. F., "Handbook of Package Engineering", McGraw Hill, 1971.

9. Kerstner, O. S., "General Principals of Package Design", NAI-57-187, Northrop Aircraft, Inc., Hawthorne, Ca, 1957.

10. Lentz, A. M., Arco Chemical Engineering Foams Technician, personal communication, October, 1990.

11. Military Standardization Handbook, Mil-HDBK-304B, "Packaging Cushion Design", United States Department of Defense, 1978.

12. Newton, E., "Fragility Assessment Theory and Test Procedure", Monterey Research Laboratory, Inc., Monterey, California, 1968.

13. Pearsons, K. S., and Ungar, E. E., "Development of Packaging Material with Constant Restoring Force", WADD TR 60-573, U. S. Air Force, Wright-Patterson AFB, Ohio, 1961.